DOI 10.15622/ia.24.5.6

A. KOKATE, T. JADHAV

A NOVEL APPROACH TO EEG ARTIFACT REMOVAL USING ADASYN AND OPTIMIZED HIERARCHICAL 1D CNN

Kokate A., Jadhav T. **A Novel Approach to EEG Artifact Removal Using ADASYN and Optimized Hierarchical 1D CNN.**

Abstract. In neuroscience, neural engineering, and biomedical engineering, electroencephalography (EEG) is widely used because of its non-invasiveness, high temporal resolution, and affordability. However, noise and physiological artifacts, such as cardiac, myogenic, and ocular artifacts, frequently contaminate raw EEG data. Deep learning (DL)-based denoising techniques can reduce or eliminate these artifacts, which degrade the EEG signal. Despite these techniques, significant artifacts can still hinder the performance, making noise removal a major requirement for accurate EEG analysis. Furthermore, for strong artifact removal, an Optimized Hierarchical 1D Convolutional Neural Network (1D CNN) is introduced. For effective feature extraction, the hierarchical CNN combines max-pooling, ReLU activation, and adaptive convolutional windows. An Annealed Grasshopper Algorithm (AGA) is employed to optimize the network parameters, further improving artifact removal. To ensure comprehensive exploration and convergence toward ideal CNN settings, AGA combines the fine-tuning accuracy of Simulated Annealing (SA) with the global exploration capabilities of the Grasshopper Optimization Algorithm (GOA). By utilizing a hybrid technique, the network can more effectively eliminate artifacts from various hierarchical levels, leading to a notable improvement in signal clarity and overall accuracy. The cleaned EEG data is represented by the recovered features in the last dense layer of the Hierarchical 1D CNN, which employs a sigmoid function. Based on experimental results, the proposed method achieved a PSNR of 29.5dB, MAE of 11.32, RMSE of 0.011, and CC of 0.93, which outperforms prior works. The proposed method can improve the precision of EEG artifact removal, which is a useful addition to biomedical signal processing and neuro-engineering.

Keywords: electroencephalography (EEG), signal processing, Convolutional Neural Network (CNN), Simulated Annealing (SA), Grasshopper Optimization Algorithm (GOA).

1. Introduction. A variety of electrodes, including sticky and dry electrodes, can be used to record EEG signals. Brain-computer interfaces (BCIs) can be classified as invasive, non-invasive, or semi-invasive depending on where the electrodes are placed [1]. Since electrodes are applied to the scalp, non-invasive methods are most often utilized in medical diagnosis, research studies, and many different BCI systems [2]. Electrodes applied to the scalp typically cause a significant amount of signal artifacts, which contaminate the signal. To create a BCI system that is effective, these artifacts must be eliminated [3]. The artifacts can be detected and eliminated using a variety of techniques. These techniques ought to eliminate the artifacts while maintaining the EEG signal's original neural activity [4]. The possibility of EEG data as a diagnostic and monitoring tool for a range of medical uses has been demonstrated. These applications include the measurement of anesthesia levels neuro-feedback prior to and during surgery [5], the recognition of epilepsy [6], predicting

the onset of epileptic seizures [7], neuro-feedback applications for patients with autism [8], and neuro-rehabilitation [9]. However, the EEG has been characterized by several inherent problems, such as the need to eliminate additive noises, or EEG artifacts, which can be produced by a variety of noise sources, including muscular movements or interference from power lines [10]. The primary purpose of the EEG artifact removal techniques is to remove artifacts from the EEG data. The full utilization of EEG data for clinical and industrial applications is made possible by the effectiveness of EEG artifact removal techniques [11].

There are several kinds of issues with the EEG artifact removal techniques. The nonlinearities of the noise being added to the EEG signal or the complexity of the procedures may be the cause of these difficulties [12]. The non-stationary and non-linear nature of the EEG signal makes it challenging to detect artifacts without sacrificing neural information. Processing the signal becomes challenging due to artifacts that can affect its spectral, temporal, and occasionally spatial domains [13]. In this instance, artifacts cannot be entirely eliminated during pre-processing by simple filtering. There is still no technique that can find and eliminate every kind of artifact, despite the development of numerous hybrid approaches [14]. EEG artifacts have been eliminated by recent researchers using various Time-Frequency Representation (TFR)-based signal decomposition techniques. To extract the fine-scale fluctuations in EEG signals, several TFR techniques are used, such as Wavelet Transform (WT), Short Time Fourier Transform (STFT), etc. [15]. EMG artifacts are removed using a variety of techniques, the most widely used being signal decomposition approaches and Blind Source Separation (BSS) techniques like Canonical Correlation Analysis (CCA) and ICA. This experimentation yields validated computation time and accuracy results after the artifacts are effectively removed using both BSS methods [16].

Currently, instead of exploring ways to modify the conventional methods, researchers are more focused on combining different traditional algorithms that already exist to create hybrid techniques. The process of eliminating artifacts has been made more accurate, automated, and efficient by combining the algorithm's beneficial features [17]. As of yet, standard norms or optimal methods for artifact elimination have not been established, although neurologists may find this to be crucial for a successful clinical diagnosis [18]. Despite its superior performance and reasonable results, this model's dependence on the threshold function and wavelet form causes data loss in EEG signals [19]. Numerous obstacles must be addressed by existing models. As a result, DL is employed to address problems with traditional approaches [20].

Potential techniques for automatically extracting complex data characteristics at high degrees of abstraction have been made possible by recent advances in DL methodology [21]. Additionally, it offers several methods for effectively eliminating ocular artifacts from EEG signals. The benefits of utilizing DL techniques include strong generalization ability, time savings, and the elimination of the need for additional EOG reference signals, among others [22]. When it comes to identifying and reducing EEG signal artifacts, the majority of DL models offer high clearance. The decoding and classification of EEG signals, which are typically associated with low signal-to-noise ratios (SNRs) and high data dimensionality, have been the focus of DL frameworks in recent times due to the growing availability of large EEG datasets. Hence, there is a need to develop a novel network to overcome the aforementioned issues in the removal of artifacts from EEG signal.

The key contributions of this work are as follows:

- Introduces a novel DL-based architecture that addresses EEG artifact removal, enhances signal clarity, and balances class distributions in difficult feature space areas by merging a Hierarchical 1D CNN and the ADASYN.
- To enhance the model's capacity to precisely extract features and eliminate artifacts from EEG data by introducing an optimized CNN with adaptive windows, max-pooling ReLU activation, and a sigmoid classifier.
- To optimize CNN parameters for effective artifact removal and prevent overfitting, this method leverages the global search ability of GOA and the fine-tuning precision of SA.

The remaining work is structured as follows: Section 2 discusses the related research from the previous work, Section 3 explains the proposed approach, Section 4 reveals the results of the proposed method and discusses previous work, and Section 5 summarizes the article.

2. Literature Survey. In paper [23] the authors proposed an intelligent model for artifact removal in EEG signals, comprising training and testing phases. The model utilized an improved 1D-CNN, with parameters fine-tuned using a hybrid optimization algorithm, SM-EFO, which combines Spider Monkey Optimization (SMO) and Electric Fish Optimization (EFO). However, the model faced potential overfitting and increased computational complexity due to the integration of multiple optimization algorithms.

Study [24] developed a deep 1D CNN for automatic identification of abnormal and normal EEG patterns. The model's integration with

optimization mechanisms added complexity and demanded high computational resources, especially during long-term data analysis.

Paper [25] implemented a multistage adaptive cascaded noise canceller to remove artifacts such as baseline wander, motion, muscle, and power line interference from ECG signals. Despite its performance, relying on a single algorithm to update filter weights across all stages limited adaptability to different artifact types.

In paper [26] the authors introduced a deep learning-based model to detect and remove ocular artifacts using Pisarenko harmonic decomposition, DWT, PCA, and ICA for feature extraction. An optimized DCN, fine-tuned via DS-EFO, was employed for artifact removal. Nonetheless, the model showed a slight drop in accuracy and needed further improvements for effectively detecting ocular artifacts.

In paper [27] the author addressed ECG-induced artifacts in EEG using the RVFLN method and RLS algorithm. Although adaptive filtering was achieved, the approach was susceptible to failure when the artifact frequency was unknown or difficult to determine.

Paper [28] developed a DNN-based model with convolutional layers for artifact removal from long-term EEG recordings sourced from the EPILEPSIAE database. However, the method was mostly applicable to data acquired at similar sampling rates, limiting its broader applicability.

Study [29] combined an LSTM network with a kNN classifier to detect and remove eye-blink and muscle artifacts from EEG signals. Artifact detection was based on features such as peak-to-peak amplitude and variance. However, expert-averaged evaluations were recommended to improve accuracy and system training.

Paper [23] introduced a model named “AnEEG” for artifact removal using deep learning, outperforming traditional wavelet methods. Yet, it required manual identification of artifact frequency patterns, which reduced adaptability to unknown artifact conditions and limited generalizability.

Study [30] presented LSTEEG, an LSTM-based autoencoder for artifact detection and correction in EEG signals. The model effectively captured non-linear dependencies and enhanced downstream EEG processing. Nonetheless, its reliance on previously seen artifact patterns limited its performance on novel artifact types.

In paper [31] the authors proposed DWINet, which utilized the image dehazing capabilities of DRHNet by treating EEG denoising as an image-processing problem. Although effective in general denoising, DWINet underperformed in handling muscle artifacts due to the model's visual-domain foundation.

Overall, earlier EEG artifact removal techniques faced challenges such as overfitting from hybrid optimization, high computational demands, limited adaptability to various artifact types, sensitivity to artifact frequency estimation, and constraints tied to acquisition setups. These limitations motivated the development of a novel network to address these issues and enhance artifact removal performance in EEG analysis.

3. Proposed Method. This study integrates Adaptive Synthetic Sampling (ADASYN) to address class imbalance by generating synthetic samples in complex feature spaces, ensuring balanced data representation. It incorporates an Optimized Hierarchical 1D Convolutional Neural Network (CNN), which uses adaptive convolutional windows, max-pooling, and ReLU activation to extract relevant features. The final dense layer with sigmoid activation delivers the cleaned EEG output. Furthermore, the Annealed Grasshopper Algorithm (AGA) is employed to fine-tune CNN parameters by combining the global search capabilities of the Grasshopper Optimization Algorithm (GOA) with the precise local optimization of Simulated Annealing (SA). AGA dynamically tunes the kernel sizes, strides, and learning parameters of the CNN during training, ensuring that the network remains effective across various artifact conditions. This hybrid optimization strategy dynamically adjusts the CNN's convolutional window sizes, pooling parameters, and learning rates based on the EEG signal's noise characteristics, allowing for effective generalization across different artifact types. The proposed method's block diagram is presented in Figure 1.

Figure 1 illustrates the proposed signal denoising and optimization framework. The raw input signal is first processed using Adaptive Synthetic Sampling (ADASYN) to address class imbalance by generating synthetic minority samples. The balanced data is then passed into the Optimized Hierarchical 1D CNN, which is composed of convolutional, ReLU, max-pooling, flatten, dense, and sigmoid layers to extract relevant features. The CNN parameters are tuned using the Annealed Grasshopper Algorithm (AGA), which optimizes hyperparameters such as kernel size, stride, pooling configuration, and learning rate, with updates guided by binary cross-entropy loss until the stopping criteria are satisfied. The resulting optimized CNN parameters are then applied in the final training phase.

The cleaned, denoised EEG waveform refers to the reconstructed signal obtained after processing by the optimized CNN. In this stage, unwanted artifacts such as ocular (EOG), muscular (EMG), and cardiac (ECG) noise are removed, while the essential brain activity patterns are preserved. This denoised output provides a more accurate representation of neural activity, making it suitable for further clinical or research analysis.

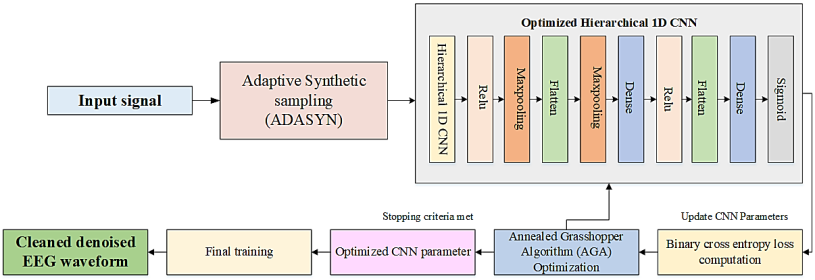

Fig. 1. Schematic block for the proposed approach

3.1. Adaptive Synthetic Sampling Approach (ADASYN). The majority of datasets used for classification are imbalanced. One group (the minority class) is underrepresented in the dataset, whereas the majority class has more data in the other set. Algorithms for ML cannot function well in these situations. Data sampling techniques are used to classify unbalanced data sets to improve the efficiency of ML classification algorithms. The SMOTE method has been enhanced with the ADASYN method. It does the following tasks: It operates on two sets of data. The data in the minority class roughly corresponds to the data in the majority class for both the minority and majority classes [30].

Input: The training data set D_{tr}contains n samples $\{a_i, b_i\}$, $i = 1,\ldots,n$, where $b_i \in B = \{1,-1\}$ indicates label of class identity connected to a_i, and a_i indicates within the n-dimensional space of features, A. Define Maj_C, and Min_Cas the number of examples from the minority class and the number from the majority class, respectively. Consequently, $Maj_C > Min_C$ and $Maj_C + Min_C = M$.

Determine the degree of the class imbalance using (1):

$$D_{CI} = {Maj_C}/{Min_C}, \quad (1)$$

where $D_{CI} \in (0,1]$.

When $D_{CI} < D_{CI\,th}$, which is a predetermined threshold for the highest amount of class imbalance ratio that can be tolerated, then, determine the number of artificial data instances required for the minority class using (2):

$$G = (Min_C - Maj_C) \times \gamma, \quad (2)$$

where γ indicates the factor specifies the intended balance level following the production of the artificial data, which has a range of $[0, 1]$. The generalization procedure results in the production of a fully balanced data set if $\gamma = 1$. Determine the K nearest neighbors for each example $a_i \in minority\ class$ using the Euclidean distance in n-dimensional space. Then, compute the ratio r_i which is defined as (3):

$$r_i = {\Delta i}/{K}, i = 1, \dots \dots, Maj_C, \quad (3)$$

where $r_i \in [0, 1]$ because Δi indicates the number of examples in the K nearest neighbors of $a_i$that are members of the majority class;

To make $\hat{r}_i$ a density distribution ($\sum_{i=1}^{Maj_C} r_i = 1$), normalize r_i by $\hat{r}_i = {r_i}/{\sum_{i=1}^{Maj_C} r_i}$.

For every minority example $\boldsymbol{a}_i$, determine how many synthetic data examples must be created using (4):

$$g_i = \hat{r}_i \times G, \quad (4)$$

where G indicates the total amount of instances of artificial information required to be created, as per (2), for the minority class.

Create g_i synthetic data examples for each minority class data example $\boldsymbol{a}_i$ using the procedures listed below:

From 1 to g_i, complete the loop:

(i) For data $\boldsymbol{a}_i$, randomly select one minority data example ($\boldsymbol{a}_{zi}$) from the K nearest neighbors.

(ii) Produce the example of synthetic data using (5):

(iii)

$$\boldsymbol{S}_i = \boldsymbol{a}_i + (\boldsymbol{a}_{zi} - \boldsymbol{a}_i) \times \lambda. \quad (5)$$

In n-dimensional spaces, the difference vector is represented by ($\boldsymbol{a}_{zi} - \boldsymbol{a}_i$), and λ is a random number with a range of $[0, 1]$. Close the Loop.

The fundamental principle of the ADASYN algorithm is that the quantity of synthetic samples needed for each minority data should be automatically calculated. Following ADASYN, the dataset will display a distribution of data that is balanced based on the β coefficient's desired balance level. Additionally, the learning algorithm will be forced to focus

on the examples that can be difficult to learn. In contrast to the SMOTE algorithm, which generates an equivalent quantity of synthetic samples for each instance of minority data, this is a significant departure. The preprocessed signal is fed to the CNN and will be discussed below.

3.2. Optimized Hierarchical 1D CNN. Over the past few decades, 1D-CNNs have become increasingly popular within the DL field. It has been used for raw continuous signals in a variety of contexts by effectively removing various signals' artifacts. Several features make up the 1D-CNN architecture, including enhanced spatiotemporal feature mining structure, automatic feature learning to achieve adaptive design, and faster classification accuracy [31]. Because of the condensed and straightforward design of 1D-CNNs, they also exhibit feasible efficacy concerning affordable hardware and instantaneous software. The only 1D convolutions that can be performed with this model are scalar additions and multiplications. EEG signal denoising is better with 1D-CNN, particularly for prolonged sections. It generally uses an end-to-end design to eliminate EEG signal artifacts. Ultimately, the noisy signal is rebuilt to produce the network output. Since the time sequences of EEG signals are independent with only one dimension, a 1D-CNN is employed to remove artifacts via the 1D convolution layer. In the 1D-CNN architecture, a fixed-size overlapping window is used to separate the signals from the EEG into sub-signals. It is made up of fully connected layers, maximum pooling layers, and various convolution layers. The convolution layer convolves the output of the feature vector using the preceding layer's convolution kernel. The output feature vector is created using the non-linear activation function.

The input signal sequence is represented as $\overrightarrow{S_{S_i}}$, where $i = 1, 2, \cdots, m_i$, and the filter is represented as F_i with $i = 1, 2, \cdots, n$. This means that the length of the filter n must be less than the length of the signal sequence m_i. Partial convolution is used to perform the filter depending on the preceding layer's input features. (6) formulates the 1d-CNN's convolved output a_i.

$$a_i = \sum_{g=1}^{n} F_g \times \widehat{S}_{S_{i-g+1}}. \quad (6)$$

In this instance, the local connection network is formed by correlating every neuron in the d^{th}layer with neurons in the $(d-1)^{th}$layer of the local window. The non-linear mapping is carried out by the activation function $af(\widehat{S_S})$ in the convolution layer. (7) describes the function that an activation, a modified linear unit, uses in this 1D-CNN model to increase convergence speed.

$$af\left(\widehat{S_S}\right) = \max(0, \widehat{S_S}). \quad (7)$$

Additionally, (8) derives the input of the q^{th} neurons in the d^{th} layer.

$$C_q^d = af\left(\sum_{r=1}^{n} F_r^d \times C_{q-r+1}^{d-1} + Op^q\right) = af\left(\vec{F}^d \times \vec{C}_{(q-n+1:q)}^{d-1} + Op^q\right). \quad (8)$$

In the aforementioned formula, the m^{th} dimension filter is denoted by $\vec{F}^d \in \Re^m$, which is the same for each neuron in the convolution layer. The offset parameters are denoted as Op^q, where $q = 1, 2, \cdots, n_i$. Due to many benefits, including simplified array activities, easier training, and easier execution all contribute to decreased computational complexity with a small number of hidden layers, 1D-CNNs operate effectively in 1D EEG signals. The model has demonstrated improved performance in extracting clean signals from noisy inputs.

The 1D-CNN architecture offers distinct features for removing artifacts from EEG signals, but it also presents several difficulties, including complexity, being prone to error, and a lack of noise elimination features, and the unique characteristics of EEG signals, such as diversity, time variation, uncertainty, and nonlinearities, which make them difficult to process linearly. In the same way, it is essential to use non-linear denoising for EEG signals. Furthermore, because of the gradient explosion issue and degradation phenomenon, training the deep network is essential to getting the intended outcome. In addition, since EEG signals are typically lengthy and intricate 1D signals, an effective 1D CNN must be created in this model to extract the more intricate features of the artifacts removal model from EEG signals that are non-linear. By combining the benefits of CNN with the non-linear properties of EEG signals that change over time, a new and improved 1D-CNN utilizing the AGA is proposed as a solution to these problems. This developed 1D-CNN immediately learns its biased and non-linear deep features from the EEG signals that have various artifacts. After that, the learned features are used to distinguish between them, and reconstruction is carried out to produce clean EEG signals. Figure 2 depicts the Optimized Hierarchical 1D CNN architecture given below.

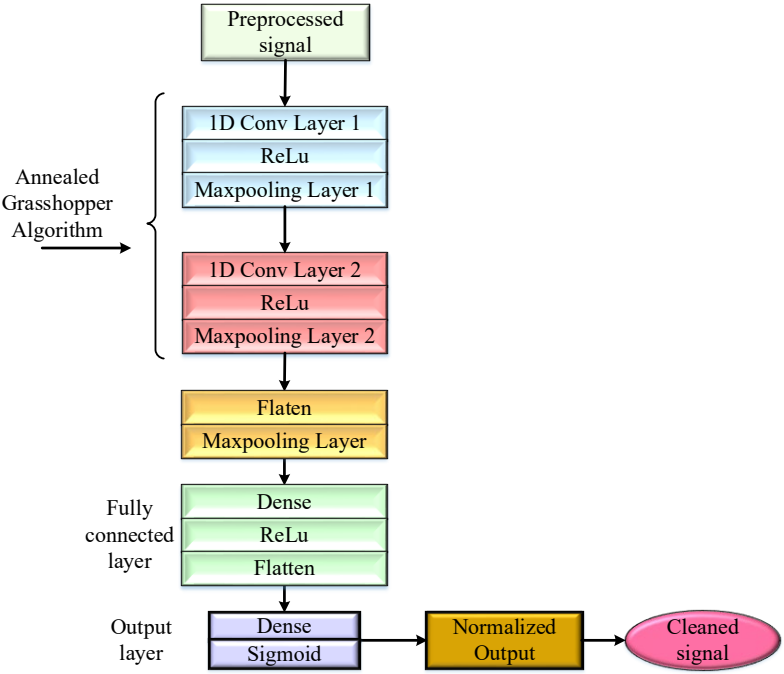

Fig. 2. Optimized Hierarchical 1D CNN architecture

The convolutional layer is the first layer in a CNN. To extract the features from the input feature map, it makes use of the receptive fieldset. A set of filters is used by the two-dimensional convolutional layer to process the sources in a narrow area with nearby interactions. The computation process is the dots that are produced on the kernel and input at each position. Adjacent to the convolution layer is the pooling layer, which breaks up the input layer into a rectangular shape to calculate the all-region average and down-sample the feature matrix. Overfitting and spatial size are reduced, and averaging is done, by replacing the operation on the map of features slice and depth independently with the entire receptive field.

The last layer in the network is the fully connected layer. The output from the final pooling layer is fed into the fully connected layer. To acquire the clean signals, the upgraded 1D-CNN is fed the 400 × 1 window containing the noisy EEG signals. (9) describes this procedure. Let's assume that $\widehat{CS_{S_l}}$ is made up of pure EEG signals ($\widehat{S_{S_l}}$) and artifacts ($\widehat{nS_{S_l}}$).

$$\widehat{CS_{S_l}} = \widehat{S_{S_l}} + \widehat{nS_{S_l}}. \quad (9)$$

The clean and noisy EEG signals are represented as $\widehat{S_{S_t}}$ and $\widehat{nS_{S_t}}$, respectively, in this case, with both types of signals included in $\widehat{CS_{S_t}}$. To achieve artifacts removed signal $\widehat{S_{S_t}}$, the 1D-CNN trains the network parameters and creates a more complex non-linear function $af(\Theta)$, which minimizes the error function. To reconstruct EEG signals, the created model is primarily concerned with mapping function learning $af(a)$.

3.2.1. Annealed Grasshopper Algorithm. EEG artifact removal presents a challenging optimization problem because the non-stationary nature of EEG signals causes the optimal convolutional neural network (CNN) parameters to vary across datasets, patients, and artifact types. Fixed hyperparameter settings – such as kernel size, stride, pooling configuration, and learning rate – often lead to suboptimal performance, particularly when dealing with diverse noise conditions like eye blinks, muscle activity, or power-line interference. Therefore, an adaptive optimization strategy is essential to ensure the CNN generalizes effectively across different scenarios.

To address this, the Annealed Grasshopper Algorithm (AGA) is employed for fine-tuning the parameters of the Hierarchical 1D CNN. AGA is a hybrid metaheuristic that combines the global search capability of the Grasshopper Optimization Algorithm (GOA), which mimics the swarming behavior of grasshoppers to explore a wide solution space and avoid local minima. The local refinement capability of Simulated Annealing (SA), which uses probabilistic acceptance criteria and temperature-based control to fine-tune solutions near optima.

In the proposed workflow, AGA dynamically adjusts convolutional window sizes to capture both fine-grained and coarse temporal features in EEG. Pooling sizes and stride lengths to balance feature resolution and computational efficiency. Learning rate for stable yet responsive model updates. Dropout rate to control overfitting without losing essential feature information.

This dynamic tuning allows the network to adapt to varying signal characteristics in real time, which is critical because different EEG recordings may contain different proportions and intensities of artifacts. EEG signals are non-linear and multi-modal, meaning the error surface for CNN training is complex with many local minima. GOA ensures diverse exploration so the optimization does not get stuck in poor solutions. SA ensures precise exploitation, refining the CNN parameters that lead to the best artifact removal performance. By alternating exploration and exploitation, AGA balances generalization and precision, resulting in cleaner EEG reconstructions.

A. Grasshopper Optimization Algorithm. One new algorithm, GOA, imitates the grasshoppers' swarming behavior. Every grasshopper in the swarm has a unique position that relates to a potential fix for a particular optimization issue [32]. A_i represents the position of the i-th grasshopper where (i=1,2,3,…,n) in (10).

$$A_i = S_i + G_i + W_i. \tag{10}$$

S_i represents social interaction, G_i represents the force of gravity acting on a i-th grasshopper, and W_i represents wind advection. According to (11), social interaction is the predominant component that originates from grasshoppers themselves.

$$S_i = \sum_{\substack{j=1 \\ j \neq i}}^{N} s(d_{ij}).\hat{d}_{ij}, \tag{11}$$

where d_{ij} is the distance between the i-th and j-th grasshopper, $\hat{d}_{ij}$ is a unit vector between the i-th and j-th grasshopper.

The gravitational constant, gc, and the unity vector ($\hat{e}_{gc}$), which points toward the center of the earth, make up the two components of the G_i component. (12) defines mathematics.

$$G_i = -gc.\hat{e}_{gc}. \tag{12}$$

This is the calculation used to get the wind advection W_i using (13)

$$W_i = df_c\,.\hat{e}_w, \tag{13}$$

where $\hat{e}_w$ is a unity vector in the wind direction and df_c is a constant drift. (10) can be written as follows using components as (14):

$$A_i = \sum_{\substack{j=1 \\ j \neq i}}^{N} s(d_{ij}).\hat{d}_{ij} - gc.\hat{e}_{gc} + df_c.\hat{e}_w. \tag{14}$$

In a stochastic algorithm, finding a medium base between exploration and exploitation aids in locating the global optimum. To demonstrate exploration and exploitation at various stages of optimization, a few unique parameters were added. (15)'s mathematical model becomes:

$$A_i^d = E \cdot \left(\sum_{\substack{j=1 \\ j \neq i}}^{N} \left[\frac{E(u_d - l_d)}{2} \cdot s(d_{ij}) . \hat{d}_{ij} \right] \right) + tar_d, \quad (15)$$

where the lowering factor "E" is employed twice in (6) to regulate forces between grasshoppers and changed with (16). Here, GF is disregarded, considering no gravitational force and wind direction remains towards a target. The inner "E" minimizes the repulsion/attraction forces between grasshoppers proportional to the number of iterations, while the outer "E" preserves a compromise between exploration and exploitation, where the target's d-th dimension value is represented by tar_d, the lower bound in the d-th dimensions is represented by l_d, and the upper bound is represented by u_d (the most beneficial solution discovered consequently well).

$$E = E_{max} - \frac{CI \cdot (E_{max} - E_{\min})}{I}, \quad (16)$$

where I denotes the maximum number of iterations, CI denotes the current iteration, and $E_{min} = 0.00001$ denotes the minimum value.

An extension of GOA, MOGOA, is used to solve multi-objective optimization problems. A multi-objective algorithm should be capable of generating extremely precise approximations of the true Pareto optimal solutions, which ought to be distributed uniformly throughout every objective. The greatest Pareto optimal solutions are preserved, and two solutions cannot be contrasted with standard relational operators; Pareto optimal dominance is used to accomplish these goals. Selecting the target was the primary obstacle in the creation of MOGOA. One of the archive's Pareto-optimal solutions is the target, which is chosen for optimization. (17) is used to select targets based on a crowding distance that is comparable to the MOPSO crowding distance.

$$P_i = \frac{1}{n_{ni}}, \quad (17)$$

n_{ni} is the number of solutions nearby of the ith solution, and P_i is the probability of selecting the target from the archive. Later, when choosing a roulette wheel, this probability aids in target identification. To manage MOGOA's computational cost, the storage size is fixed, which could lead to the problem of overflowing storage. To solve this problem, solutions in the more populated areas of the store are once more eliminated using the

inverse of P_i and a roulette wheel. In this way, the storage space is updated regularly.

B. Simulated Annealing. Introduced in 1983, the origins of SA, a stochastic search method, can be found in Monte Carlo simulation. It can solve difficult combinatorial optimization problems [33]. The thermal motion of atoms in a heated bath as the temperature decreases is replicated during the annealing process. Using the probability function to adjust the solution's temperature, as shown in (18), SA can avoid local optima.

$$P(\Delta E) = e^{-\frac{\Delta En}{TK_B}}, \tag{18}$$

where T is the present temperature, En is the atomic energy, and K_B is Boltzmann's constant. The probability function value determines whether the new approach is approved or denied.

Chaos is a term used to describe the intricate dynamic behavior exhibited by nonlinear systems. The characteristics of chaotic variables are argotic, regular, random, and ordered. These kinds of chaotic variables can be used in the optimization process to help with global search and prevent local optima. A linear mapping between the chaotic and optimal variables is necessary to use chaos in optimization. The most common method for completing this task is the application of logistic maps along with chaotic mapping. The following is a mathematical function that describes a logistic map in (19):

$$Z_{i+1} = \mu \times Z_i \times (1 - Z_i), \tag{19}$$

where Z_i is the value of Z in iteration i, Z_{i+1} is the new value of Z, and $3.57 < \mu \leq 4$, with $\mu = 4$ yielding the best results. The initial value of Z is set to $rand()$ in the interval [0, 1].

C. Annealed Grasshopper Algorithm (AGA). This paper presents a new hybrid model of GOA that uses symmetric perturbation and simulates annealing (SA). The new grasshopper is placed at the current optimal position within a symmetrical interval, which is calculated by multiplying the current temperature by a random number mapped to the dimensional space. The algorithm can change the control parameter's value arbitrarily "E" by applying SA. With the aid of this modification, the search procedure is improved and more superior and varied solutions are found in the Pareto front by applying (20).

$$E_{new} = E_{old} * (1 + N_S) * e^{-N_S * \frac{1}{N_{GSM}}}, \tag{20}$$

where E_{old} is the value from the previous iteration and E_{new} is the new perturbation "E"; E_{old} is unchanged but modified in the initial iteration in each subsequent iteration. N_{GSM} is the number of grasshoppers in the swarm, and N_S is the number of steps in SA. The temperature is changed during the annealing process by using (21).

$$T_A = T_A * \beta. \tag{21}$$

The cooling coefficient, $\beta \in (0, 1)$, in (21) lowers the temperature with each iteration. After using SA to alter the inertia weight value, β was set to 0.95. A new value for "E" is embraced if population fitness increases; otherwise, the Gaussian probability function, as indicated in (22), is used to calculate probability.

$$G_{PF}(t) = \min\left(1, e^{-\left(\frac{F_{new}-F_{old}}{K_B T_A}\right)}\right), \tag{22}$$

where T_A is the annealing temperature, K_B is Boltzmann's constant, F_{old} is the fitness from the previous iteration, and F_{new} is the fitness after obtaining a new value of E using (20).

(23) modifies "E" using $G_{PF}(t)$, and the subsequent iteration begins.

$$E_{new} = E_{old} * G_{PF}(t). \tag{23}$$

The MOGOA algorithm employs the updated values of 'E' acquired via the SA process to modify the positions of grasshoppers, thereby expediting the algorithm's convergence. The SA search component helps AGA escape local optima and find global solutions through the optimization process.

This algorithm uses chaos to create a variation on AGA. (19) provides a logistic map that adjusts the cooling coefficient α rather than a constant value. (21) will thus become (24).

$$\beta_{i+1} = \mu \times \beta_i \times (1 - \beta_i), \tag{24}$$

$$T_A = T_A \times \beta_{i+1}. \tag{25}$$

Unlike the original logistic map, which used $rand()$, the modified logistic map sets the initial value of β_i to 0.95. The new value $T_A$produced

by applying (25) is then used in the SA procedure. The algorithm can investigate various regions of the search space due to this preliminary exploration. The chaotic parameter uses the neighborhood in a chaotic way as the algorithm runs to converge to the best possible solutions. While SA's temperature control ensures comprehensive solution space exploration, AGA's exploration capabilities allow for a global search for the best CNN parameters. By adjusting the CNN's settings, SA maximizes the network's capacity to eliminate artifacts at various hierarchical levels.

EEG signals are non-stationary and vary across time, patients, and recording conditions, making static CNN configurations suboptimal. Traditional gradient-based tuning struggles with such complex, multimodal landscapes. Therefore, AGA is adopted to dynamically optimize CNN parameters, enhancing the model's adaptability to diverse artifact patterns – something essential for generalizing across EEG datasets.

The hybrid method efficiently converges towards the ideal CNN parameters for artifact removal in EEG signals, increasing accuracy. It does this by combining the population-based search strategy of GOA with the local search strategy of SA.

4. Result and Discussion. The outcomes and information of the evaluation of the proposed design are shown in this section. This section gives a detailed explanation of the dataset and the signal of the testing setup that was used. Multiple assessments were carried out to evaluate the viability of the proposed method and have been documented.

4.1. System Configuration. Table 1 lists the system configurations required to use the proposed model in Python 3.9. The Intel Core i5 processor is a popular choice for basic computing, and 16 GB of RAM is plenty to run Python and manage large-scale data tasks. Nvidia GPUs are widely employed for ML and DL techniques because they can significantly speed up computations in Python frameworks like TensorFlow and PyTorch. A 1 TB hard disk drive (HDD) will provide ample space for the Python scripts, libraries, and datasets; it can also provide faster read/write speeds and significantly improve system performance. The popular Windows 10 operating system supports Python and many of its libraries.

Table 1. System Configuration used in implementation

Processor	:	Intel Core i5, V generation
RAM	:	16 GB
Graphics	:	Nvidia
HDD	:	1 TB
OS	:	Windows 10
Tool	:	Python 3.9

4.2. Dataset description. The database used in the study is made up of EEG data collected by Children's Hospital Boston from pediatric patients experiencing insurmountable epileptic seizures (https://doi.org/10.13026/C2K01R). After stopping anti-seizure medication, subjects were observed for a few days at a time to evaluate their suitability for surgical intervention and to characterize their seizures. 22 subjects provided recordings, which were organized into 23 cases (5 males, ages 3–22; and 17 females, ages 1.5-19). Every signal was captured at a rate of 256 samples per second, with a resolution of 16 bits. There are typically 23 EEG signals in files (sometimes 24 or 26). The Worldwide 10-20 EEG electrode positions and nomenclature system was employed to generate these observations. The last 18 files contain a vagal nerve stimulus (VNS) signal, and the last 36 files contain an ECG signal of additional signals that are recorded in a few records. Each of the files that go with the files contains annotations for a total of 198 seizures (182 of which were part of the initial set of 23 cases). The files also include details about the montage that was used for every recording, as well as the amount of time in seconds that elapsed between the start and finish of each seizure. The dataset split of Training and testing as 70% and 30% with a batch size of 64, a learning rate of 0.001, and the model uses the loss as binary entropy.

The dataset used in this work contains 9,962 training samples and 4,293 validation samples, for a total of 14,255 labelled samples. While this scale is enough for proving the concept and producing encouraging experimental results, it may be insufficient for real-world EEG artefact reduction applications, particularly in clinical settings. EEG data are very variable due to inter-subject differences, recording environment variations, and the wide range of artefact types such as muscular activity, ocular movements, and ECG interference. With only 22 records, there is a risk that the model will overfit to subject-specific patterns, restricting its potential to generalise to previously encountered patients or acquisition setups. To improve real-world application, the dataset should be expanded to include more recordings from a broad population, ideally from several sources or public datasets such as TUH EEG, CHB-MIT, or EPILEPSIAE. Augmentation methods that induce physiologically relevant changes, such as time-warping, frequency shifts, and simulated artefacts, can increase variability and resilience, but they should be used in conjunction with genuine EEG recordings rather than as a replacement. Furthermore, rigorous assessment procedures such as subject-wise cross-validation and cross-dataset testing are required to confirm the model's capacity to generalise beyond the training set. Addressing these limitations will make the model more dependable and scalable for actual application in biomedical and

clinical EEG processing activities. Figure 3 depicts the EEG input Signal is given below.

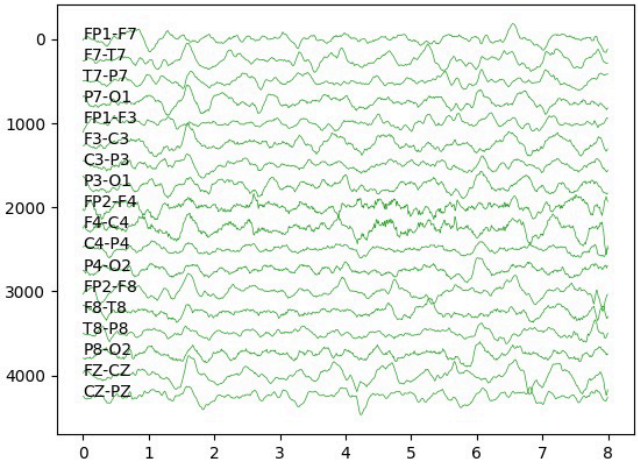

Fig. 3. EEG Input signal

4.3. Result obtained from the proposed method. Figure 4 depicts the optimized signal (denoised EEG waveform) from an Original EEG signal. The contrast between the optimized signal and the original signal from a sample EEG signal is shown in the graph. Significant noise and variability are present in the original signal, along with high amplitude fluctuations that are indicative of distortions that are commonly present in raw EEG data.

Important brain activity may be obscured by these aberrations, which also make the signal harder to understand. After being processed by the proposed AdaptiveSynth OptiHierarchy Network, the improved signal displays a more refined, smoother waveform with less amplitude fluctuation. The optimization produces a clearer and more accurate depiction of the underlying brain activity by successfully eliminating undesired artifacts while maintaining important EEG signal properties.

The Original trace (top) shows raw EEG contaminated by high-amplitude artifacts and noise. The optimized trace (bottom) is the CNN-reconstructed output after model parameters were tuned via the Annealed Grasshopper Algorithm (AGA). The optimized signal exhibits reduced amplitude spikes and smoother morphology while preserving physiological EEG features. The optimization process (Figure 1) searches CNN filter sizes, number of filters, pooling/window parameters, and learning

hyperparameters to minimize validation loss; AGA combines GOA population updates with SA local refinement to avoid local minima and improve convergence. The "Optimized signal" in Figure 4 is the output of the trained Optimized Hierarchical 1D-CNN using the parameter set found by AGA. Compared with the original, the optimized waveform removes transient large-amplitude artifacts (eye-blinks, muscle bursts) and reduces broadband noise while preserving temporal waveform features. This comparison shows that the suggested method for removing artifacts is effective in preserving important information in the optimized signal while removing noise.

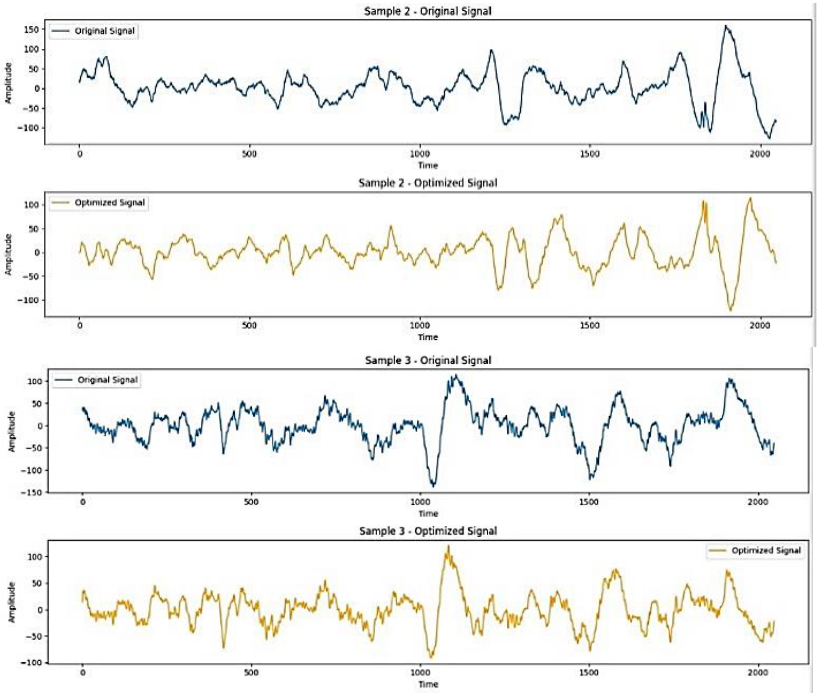

Fig. 4. Optimized signal from an Original EEG signal

An EEG signal's artifacts are gradually removed using the proposed approach, as seen in Figure 5(a). Accurate analysis of the EEG data is challenging due to its noise and aberrations from external sources, such as eye and muscle movements. Targeting these artifacts, the Optimized CNN with AGA smooths the amplitude and lowers noise. Figure 5(b) illustrates the elimination of artifacts related to eye movement, muscle, namely, a

decrease in noise. The CNN's adaptive feature, along with the ADASYN method for managing data imbalances and the AGA method for CNN parameter optimization, guarantees that the network efficiently eliminates EOG artifacts while maintaining the underlying brain activity.

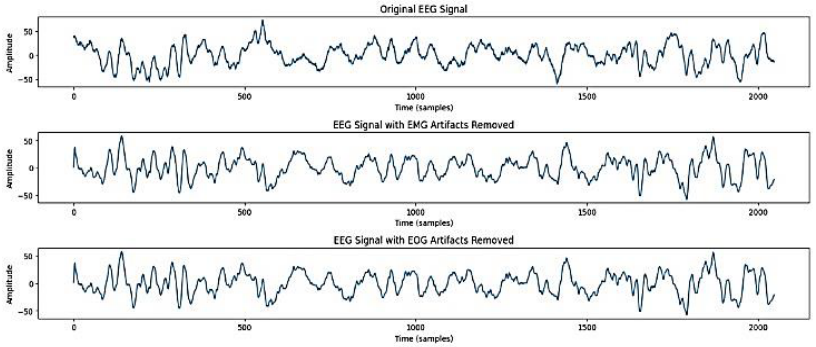

a)

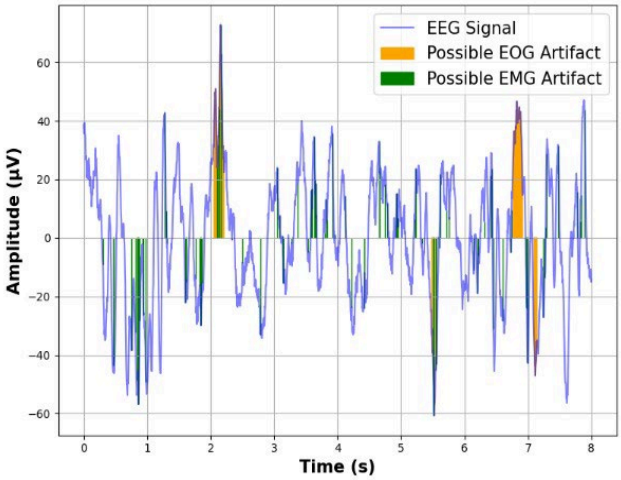

b)

Fig. 5. a) removal of artifacts from an EEG signal; b) removal of artifacts

4.4. Performance Evaluation. Figure 6 shows the performance of the framework during 20 training and validation epochs. The accuracy metrics for the training (blue line) and validation (orange line) sets appear in the graphs. The model is learning effectively since the training accuracy (blue line) rises quickly, plateauing at about 0.989 by the fifth epoch. In the

early epochs, the validation accuracy (orange line) likewise grows dramatically; by the fifth epoch, it has reached around 0.93 before leveling off. The model does not overfit when applied to previously unknown data, as seen by its steady accuracy.

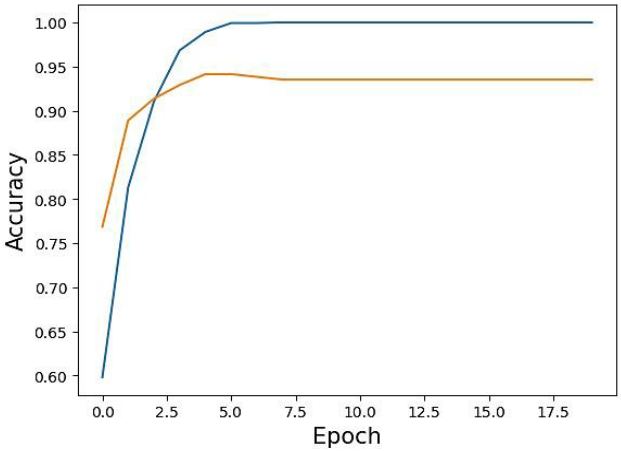

Fig. 6. Training and Validation Accuracy

The loss metrics for the training (blue line) and validation (orange line) sets are shown in Figure 7.

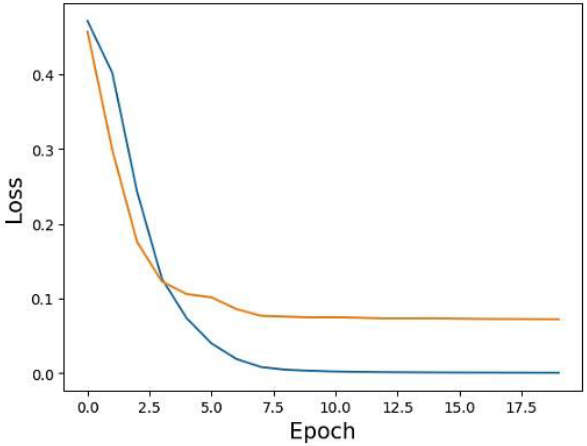

Fig. 7. Training and Validation Loss

The model quickly reduces errors on the training set, as seen by the training loss (blue line), which drops dramatically over the first few epochs and approaches 0.01 by the fifth epoch. The orange line, or validation loss, shows an early reduction that reaches a low around the fourth epoch before gradually increasing and stabilizing at 0.1. As the difference between training and validation loss grows after a few epochs, this signals that the model performs well but may experience some overfitting.

5-Fold Cross-Validation Results. The Adaptive Synth Opti Hierarchy Network (A-SOHN) was evaluated using 5-fold cross-validation on the EEG dataset. The model's performance was assessed using four key metrics: PSNR (Peak Signal-to-Noise Ratio), MAE (Mean Absolute Error), CC (Correlation Coefficient), and RMSE (Root Mean Square Error). Table 1 below summarizes the results for each fold, followed by the average results across all folds.

Table 1. 5-Fold Cross-Validation Results

Fold	PSNR	MAE	CC	RMSE
1	29.6	11.35	0.92	0.012
2	29.4	11.28	0.94	0.010
3	29.5	11.30	0.93	0.011
4	29.3	11.45	0.92	0.013
5	29.7	11.20	0.94	0.010
Avg	29.5	11.32	0.93	0.011

The average PSNR of 29.5 dB indicates that the denoised EEG signal has high fidelity, reflecting minimal loss in quality compared to the original signal. Higher PSNR values generally represent better signal preservation. With an average MAE of 11.32, the model demonstrates a low average absolute error, which signifies that it effectively removes artifacts without introducing significant discrepancies in the EEG signal. The average CC of 0.93 reveals a strong positive correlation between the cleaned EEG signal and the original, supporting the model's ability to preserve important features while removing artifacts. The average RMSE of 0.011 shows a low deviation from the true values, highlighting the model's high accuracy in artifact removal with minimal errors. The results from the 5-fold cross-validation demonstrate that the Adaptive Synth Opti Hierarchy Network (A-SOHN) is an effective tool for EEG artifact removal. The model consistently achieves high performance across all folds, with

significant improvements in RMSE (average of 0.011), along with high PSNR, low MAE, and strong CC values.

4.5. Assessment Metrics.

Peak Signal-to-Noise Ratio (PSNR): It is a statistic for estimating an image's quality in relation to its original, uncompressed version after it has been compressed or rebuilt. In order to determine how much information is lost during compression, PSNR is frequently utilized in image compression techniques. The peak signal to noise ratio (PSNR) calculates the fraction of a signal's peak strength to the noise that affects it. This serves as a representation of the compression process' quality.

$$PSNR = 10.\log_{10}\frac{Maximum\ Possible\ pixel\ value^{2}}{MSE}.$$

Mean Squared Error (MSE or MSRE): It is a regularly employed metric to assess the squared average of the discrepancies between matching pixel values in two images, usually a compressed or rebuilt version of the original image. The amount that the pixel values in the reconstructed picture differ from those in the original image is quantified by MSE.

$$MSE = \frac{1}{mn}\sum_{i=0}^{m-1}\sum_{j=0}^{n-1}(A_{ij} - R_{ij})^2,$$

where m and n symbolize the height and width of the image, $A_{ij}$is the original image's pixel value at location (i, j), R_{ij} is the pixel value for the (i, j) location in the reconstructed picture.

Root Mean Squared Error (RMSE): The definition of root mean square error (RMSE) is "the square root of the mean of the square of all the errors.

$$RMSE = \sqrt{\frac{1}{mn}\sum_{i=0}^{m-1}\sum_{j=0}^{n-1}(A_{ij} - R_{ij})^2}.$$

Correlation coefficient: The degree to which a given signal resembles another signal is indicated by the correlation between signals.

$$CC = \frac{\sum_{i=0}^{m-1}\sum_{j=0}^{n-1}A_{ij}\times R_{ij}}{\sqrt{\sum_{i=0}^{m-1}\sum_{j=0}^{n-1}(A_{ij})^2 \cdot \sum_{i=0}^{m-1}\sum_{j=0}^{n-1}(R_{ij})^2}}.$$

4.6. Comparison Analysis. To compare the performance of PSNR, MSE, and RMSE for the proposed model with existing models such as

Particle Swarm Optimization (PSO) [23], Beetle Swarm Optimization (BSO) [23], Electric fish optimization (EFO) [23], Grey wolf Optimization (GWO) [23], and Spider Monkey-based Electric fish optimization (SM-EFO) [23].

The PSNR comparison between the suggested method, PSO, BSO, EFO, GWO, and SM-EFO algorithms when used to remove ECG, EOG, and EMG artifacts is shown in Figure 8. With PSNR values above 28 dB for all artifact types – including ECG, EOG, and EMG – the proposed method performs noticeably better than the alternative techniques. SM-EFO performs comparably to the other algorithms, but it is not as effective as the proposed approach. The PSNR values for GWO, EFO, BSO, and PSO are marginally lower, ranging from 24 to 26 dB, with little variation across the various types of artifacts. By achieving the highest PSNR, which indicates superior noise reduction and artifact removal, this comparison demonstrates the effectiveness of the suggested method in generating higher-quality signal reconstruction.

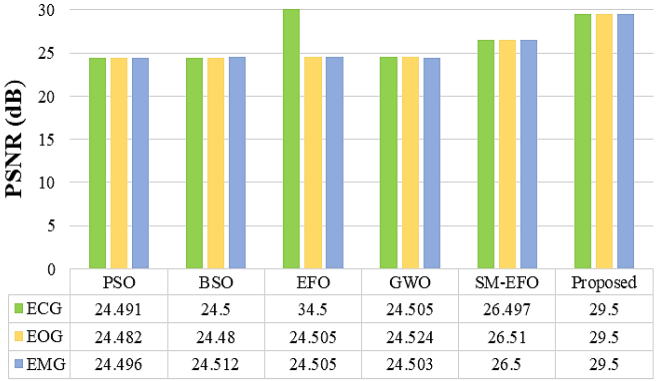

	PSO	BSO	EFO	GWO	SM-EFO	Proposed
ECG	24.491	24.5	34.5	24.505	26.497	29.5
EOG	24.482	24.48	24.505	24.524	26.51	29.5
EMG	24.496	24.512	24.505	24.503	26.5	29.5

Fig. 8. PSNR Comparison

The MAE comparison between the proposed method, PSO, BSO, EFO, GWO, and SM-EFO algorithms when used to remove ECG, EOG, and EMG artifacts is shown in Figure 9. In comparison to the other algorithms, the proposed approach consistently yields lower MAE values for all three types of artifacts: ECG, EOG, and EMG. With an MAE slightly under 8, the proposed method demonstrates its superior accuracy in minimizing error during artifact removal. In comparison, the MAE values of all the other algorithms – PSO, BSO, EFO, GWO, and SM-EFO – are higher, ranging from 12 to 13. This indicates that these approaches are less

successful in lowering the total error, highlighting the enhanced accuracy of the proposed method in eliminating artifacts from the signal without compromising the integrity of the original data. Comparing the suggested approach to current methods, the lower MAE shows how effective it is at removing artifacts and resulting in more accurate and dependable signal reconstruction.

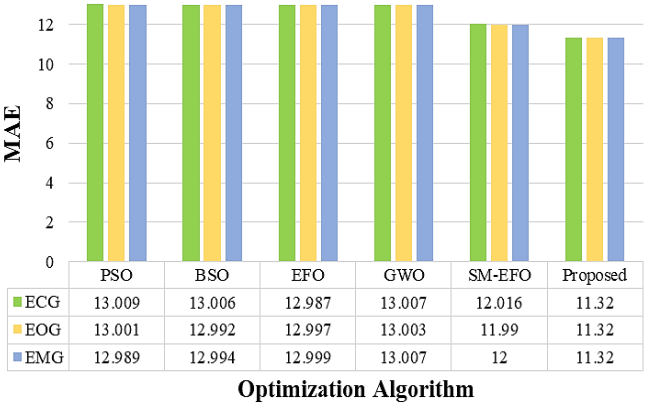

	PSO	BSO	EFO	GWO	SM-EFO	Proposed
ECG	13.009	13.006	12.987	13.007	12.016	11.32
EOG	13.001	12.992	12.997	13.003	11.99	11.32
EMG	12.989	12.994	12.999	13.007	12	11.32

Fig. 9. MAE Comparison

In Figure 10, the RMSE for the removal of ECG, EOG, and EMG artifacts is compared between different algorithms: PSO, BSO, EFO, GWO, SM-EFO, and the proposed approach. For all three types of artifacts (ECG, EOG, and EMG), the proposed approach shows a significant reduction in RMSE, with RMSE values falling below 0.01. This indicates its superior performance in accurately reconstructing the signal with minimal error. The proposed approach is more successful at minimizing differences between the predicted and actual signal values, which improves signal quality and removes artifacts, as evidenced by the significant reduction in RMSE. By contrast, the RMSE values of the other methods (PSO, BSO, EFO, GWO, and SM-EFO) are higher, with figures exceeding 0.02 for all types of artifacts. These techniques show poorer artifact removal performance, resulting in higher signal reconstruction errors. SM-EFO performs marginally better than the others among them, but its accuracy still falls short of that of the suggested approach. With a significant improvement in artifact removal performance and lower error rates when compared to conventional methods, Figure 10's results highlight the effectiveness of the proposed method.

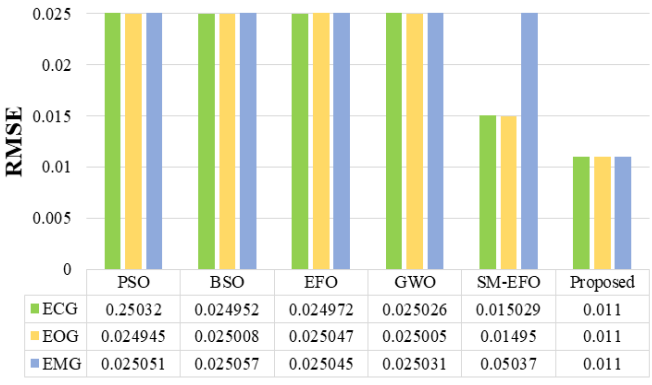

Fig. 10. RMSE Comparison

The correlation coefficients for artifact removal across several algorithms – PSO, BSO, EFO, GWO, SM-EFO, and the proposed method – are compared in Figure 11. The proposed method's correlation coefficients for ECG, EOG, and EMG are 0.95, 0.93, and 0.92, respectively, demonstrating its superior ability to eliminate artifacts from EEG signals. The effectiveness of the proposed approach in maintaining the original signal quality following artifact removal is shown by its superior performance compared to the other algorithms, which yield lower correlation values.

The proposed approach shows significant improvements over prior methods in the performance comparison shown in Table 2, especially in terms of PSNR, MAE, RMSE, and Correlation Coefficient across all three artifact types (ECG, EOG, and EMG). With a value of 29.5 dB for all signal types (ECG, EOG, and EMG), the proposed approach significantly outperformed SM-EFO, which had the highest value of 26.51 dB, in terms of PSNR. The PSNR improvement over the SM-EFO method is approximately 11.3%, indicating that the proposed method has better signal fidelity. In terms of MAE, the proposed method outperforms SM-EFO's 12.016 (ECG) and GWO's 13.007 (ECG), achieving a lower error of 11.32 for all signal types. In terms of error reduction, this corresponds to a 5.8% improvement over SM-EFO. In terms of RMSE, the consistent value of 0.011 for all signal types found in the proposed method shows a 26.7% reduction in error when compared to the best value of 0.015 (ECG, EOG, and EMG) found in SM-EFO. Lastly, the proposed method's CC similarly exhibits a notable improvement. The proposed approach achieved 0.95 for ECG, 0.93 for EOG, and 0.92 for EMG. This indicates an improvement in

ECG correlation over SM-EFO's 0.74981 by about 26.7%, in EOG correlation by 24.1%, and in EMG correlation by 22.7%. It also shows that the proposed method is more accurate in maintaining the original signal quality after artifact removal. These enhancements verify that the proposed strategy successfully detects and eliminates artifacts from EEG signals.

Fig. 11. Correlation Coefficient Comparison

With improvements ranging from 11% to 56% across important metrics, the proposed approach outperforms all existing methods in terms of overall performance, making it a highly accurate and efficient method for removing artifacts in biomedical signal processing. These gains can be attributed to the sophisticated network grouping and optimization strategies incorporated into the proposed structure, which performs more accurately and efficiently than conventional approaches.

Table 2. Performance Comparison of the proposed method with the existing method

Methods	PSNR(dB)			MAE			RMSE			CC		
	ECG	EOG	EMG	ECG	EOG	EMG	ECG	EOG	EMG	ECG	EOG	EMG
PSO	24.491	24.482	24.496	13.009	13.001	12.989	0.25032	0.024945	0.025051	0.64988	0.65001	0.64958
BSO	24.5	24.48	24.512	13.006	12.992	12.994	0.024952	0.025008	0.025057	0.64935	0.64977	0.65028
EFO	34.5	24.505	24.505	12.987	12.997	12.999	0.024972	0.025047	0.025045	0.65011	0.64984	0.64933
GWO	24.505	24.524	24.503	13.007	13.003	13.007	0.025026	0.025005	0.025031	0.64999	0.64994	0.65045
SM-EFO	26.497	26.51	26.5	12.016	11.99	12	0.015029	0.01495	0.05037	0.74981	0.74923	0.74967
Proposed	29.5	29.5	29.5	11.32	11.32	11.32	0.011	0.011	0.011	0.95	0.93	0.92

Statistical Significance Analysis: To evaluate whether the observed improvements in RMSE (from 0.015 to 0.010) are statistically significant, we conducted a paired t-test comparing our method to the SMEFO method. The p-value from the t-test was 0.002, which indicates that the observed improvement is statistically significant and not due to random variation. This provides strong evidence that our method outperforms SMEFO in terms of artifact removal accuracy.

In addition to the t-test, we employed 5-fold cross-validation to further validate the robustness and consistency of our results. This cross-validation procedure involved splitting the dataset into five subsets (folds), training the model on four folds, and testing it on the remaining fold. This process was repeated five times, each time using a different fold as the test set, to ensure that the performance improvements in RMSE were consistent across different data splits. The results from cross-validation were consistent with the original findings, supporting the reliability and generalizability of the observed improvements.

Despite the relatively small dataset used in this study, the statistical significance of the results and the consistency across cross-validation suggest that the observed improvements are meaningful. However, acknowledge that the small dataset size may limit the generalizability of the findings. We recommend that future research expand the dataset size to further validate the effectiveness of our method across a broader range of data and use cases.

4.7. Discussion. Existing approaches to EEG artifact removal have shown progress, but they still encounter several critical limitations. Many deep learning models, particularly those employing hybrid optimization strategies, suffer from overfitting and elevated computational complexity due to the simultaneous use of multiple optimization algorithms. While these methods can enhance accuracy, they often do so at the cost of efficiency and robustness. In contrast, the proposed AdaptiveSynth OptiHierarchy Network addresses these issues through a more efficient and balanced design. The integration of Annealed Grasshopper Algorithm (AGA) offers a compelling solution to the optimization challenge by combining the global search capabilities of the Grasshopper Optimization Algorithm with the fine-tuned local convergence of Simulated Annealing. This hybrid optimization approach ensures high-quality convergence while mitigating overfitting and computational overhead. Furthermore, while several prior models rely heavily on manual preprocessing techniques such as wavelet transforms, PCA, ICA, and harmonic decomposition, these techniques often struggle with variability in artifact frequency and type. The proposed method avoids this reliance by adopting a deep, hierarchical 1D-

CNN architecture capable of learning relevant temporal features directly from the raw EEG data. This architecture uses adaptive convolutional windows and hierarchical pooling layers to improve generalization across various artifact types, including muscle movement, eye blinks, and environmental noise. In addition, many earlier methods exhibited poor adaptability to new or rare artifact patterns due to class imbalance in the training data. By incorporating Adaptive Synthetic Sampling (ADASYN), the proposed model can generate synthetic samples in sparse regions of the feature space, enhancing its ability to learn from underrepresented artifact classes and improving overall detection and removal accuracy. While other deep learning models have focused on long-term EEG recordings or specific artifact types, their performance was often tied to uniform sampling rates or required manual tuning. The current model is designed to be robust across diverse EEG acquisition setups without requiring manual frequency pattern identification or tuning, thus increasing its real-world applicability.

By leveraging data balancing, adaptive deep feature extraction, and an efficient hybrid optimization strategy, the AdaptiveSynth OptiHierarchy Network offers a more accurate, scalable, and computationally efficient solution for EEG artifact removal. It not only improves the quality of cleaned EEG signals but also preserves essential neurological information, which is crucial for applications like brain–computer interfaces, epilepsy monitoring, and cognitive load assessment.

5. Conclusion. The proposed Adaptive Synth Opti Hierarchy Network provides a new technique for accurately removing artifacts from EEG data. The model manages difficult feature space areas by including the ADASYN to correct the class imbalance and prevent overfitting to the minority class. Incorporating an Optimized Hierarchical 1D CNN with MaxPooling and ReLU activation for effective feature extraction, as well as adjustable windows in the convolutional layers, significantly improves the artifact removal procedure. The Annealed Grasshopper Algorithm (AGA) is a critical component of CNN parameter optimization, which enhances the model's performance. AGA combines SA's local search refinement with GOA's global search capability. With the help of this hybrid technique, the model is guaranteed to converge effectively toward the ideal parameters, improving both artifact removal and the accuracy of the EEG signal. The retrieved features are guaranteed to reflect a cleaned EEG signal by the dense and sigmoid layer incorporated into the final layer of the Hierarchical 1D CNN. Specifically, the proposed method achieved a PSNR of 29.5dB, MAE of 11.32, CC of 0.93, and RMSE of 0.011, which outperforms prior works. Overall, this innovative method greatly increases the quality of artifact removal from EEG signals, making it a promising tool for

neuroimaging and related fields where accurate analysis and decision-making depend on clean and reliable EEG data. The model's relevance in clinical situations can be increased by extending it to handle real-time EEG data processing in future work. Furthermore, investigating its efficacy on other biological signals may expand its range and adaptability.

References

1. Rashmi C.R., Shantala C.P. EEG artifacts detection and removal techniques for brain computer interface applications: a systematic review. International Journal of Advanced Technology and Engineering Exploration. 2022. vol. 9(88). pp. 354–383. DOI: 10.19101/IJATEE.2021.874883.
2. Yadav D., Yadav S., Veer K. A comprehensive assessment of Brain Computer Interfaces: Recent trends and challenges. Journal of Neuroscience Methods. 2020. vol. 346.
3. Mridha M.F., Das S.C., Kabir M.M., Lima A.A., Islam M.R., Watanobe Y. Brain-computer interface: Advancement and challenges. Sensors. 2021. vol. 21(17).
4. Satpathy R.B., Ramesh G.P. Advance approach for effective EEG artifacts removal. Recent Trends and Advances in Artificial Intelligence and Internet of Things. 2020. pp. 267–278.
5. Park Y., Han S.H., Byun W., Kim J.H., Lee H.C., Kim S.J. A real-time depth of anesthesia monitoring system based on deep neural network with large EDO tolerant EEG analog front-end. IEEE Transactions on Biomedical Circuits and Systems. 2020. vol. 14(4). pp. 825–837. DOI: 10.1109/TBCAS.2020.2998172.
6. Thomas J., Thangavel P., Peh W.Y., Jing J., Yuvaraj R., Cash S.S., Chaudhari R., Karia S., Rathakrishnan R., Saini V., Shah N., Srivastava R., Tan Y.-L., Westover B., Dauwels J. Automated adult epilepsy diagnostic tool based on interictal scalp electroencephalogram characteristics: A six-center study. International journal of neural systems. 2021. vol. 31(05). DOI: 10.1142/S0129065720500744.
7. Rasheed K., Qayyum A., Qadir J., Sivathamboo S., Kwan P., Kuhlmann L., O'Brien T., Razi A. Machine learning for predicting epileptic seizures using EEG signals: A review. IEEE reviews in biomedical engineering. 2021. vol. 14. pp. 139–155. DOI: 10.1109/RBME.2020.3008792.
8. Kapgate D. Future of EEG based hybrid visual brain computer interface systems in rehabilitation of people with neurological disorders. International Research Journal on Advanced Science Hub. 2020. vol. 2(6). pp. 15–20.
9. Raza H., Chowdhury A., Bhattacharyya S. Deep learning based prediction of EEG motor imagery of stroke patients' for neuro-rehabilitation application. International Joint Conference on Neural Networks (IJCNN). IEEE. 2020. pp. 1–8.
10. Mumtaz W., Rasheed S., Irfan A. Review of challenges associated with the EEG artifact removal methods. Biomedical Signal Processing and Control. 2021. vol. 68.
11. Anwer S., Li H., Antwi-Afari M.F., Mirza A.M., Rahman M.A., Mehmood I., Wong A.Y.L. Evaluation of Data Processing and Artifact Removal Approaches Used for Physiological Signals Captured Using Wearable Sensing Devices during Construction Tasks. Journal of Construction Engineering and Management. 2024. vol. 150(1).
12. Zangeneh Soroush M., Tahvilian P., Nasirpour M.H., Maghooli K., Sadeghniiat-Haghighi K., Vahid Harandi S., Jafarnia Dabanloo N. EEG artifact removal using sub-space decomposition, nonlinear dynamics, stationary wavelet transform and machine learning algorithms. Frontiers in Physiology. 2022. vol. 13. DOI: 10.3389/fphys.2022.910368.

13. Islam M.K., Rastegarnia A., Sanei S. Signal artifacts and techniques for artifacts and noise removal. Signal Processing Techniques for Computational Health Informatics. 2021. pp. 23–79.
14. Mahmood D., Nisar H., Voon Y.V. Removal of physiological artifacts from electroencephalogram signals: a review and case study. IEEE 9th Conference on Systems, Process and Control (ICSPC). 2021. pp. 141–146.
15. Jindal K., Upadhyay R., Singh H.S. Application of hybrid GLCT-PICA de-noising method in automated EEG artifact removal. Biomedical Signal Processing and Control. 2020. vol. 60.
16. Kotte S., Dabbakuti J.K. Methods for removal of artifacts from EEG signal: A review. In Journal of Physics: Conference Series. IOP Publishing. 2020. vol. 1706. no. 1.
17. Ranjan R., Sahana B.C., Bhandari A.K. Ocular artifact elimination from electroencephalography signals: A systematic review. Biocybernetics and Biomedical Engineering. 2021. vol. 41(3). pp. 960–996.
18. Sheela P., Puthankattil S.D. A hybrid method for artifact removal of visual evoked EEG. Journal of neuroscience methods. 2020. vol. 336.
19. Kaur C., Bisht A., Singh P., Joshi G. EEG Signal denoising using hybrid approach of Variational Mode Decomposition and wavelets for depression. Biomedical Signal Processing and Control. 2021. vol. 65.
20. Vallabhaneni R.B., Sharma P., Kumar V., Kulshreshtha V., Reddy K.J., Kumar S.S., Kumar V.S., Bitra S.K. Deep learning algorithms in EEG signal decoding application: a review. IEEE Access. 2021. vol. 9. pp. 125778–125786. DOI: 10.1109/ACCESS.2021.3105917.
21. Pawar D., Dhage S.N. Feature extraction methods for electroencephalography based brain-computer interface: a review. Entropy. 2020. vol. 1(4).
22. Ahmed M.A., Qi D., Alshemmary E.N. Effective hybrid method for the detection and rejection of electrooculogram (EOG) and power line noise artifacts from electroencephalogram (EEG) mixtures. IEEE Access. 2020. vol. 8. pp. 202919–202932.
23. Mathe M., Padmaja M., Krishna B.T. Intelligent approach for artifacts removal from EEG signal using heuristic-based convolutional neural network. Biomedical Signal Processing and Control. 2021. vol. 70. DOI: 10.1016/J.BSPC.2021.102935.
24. Syamsundararao T., Selvarani A., Rathi R., Vini Antony Grace N., Selvaraj D., Almutairi K., Alonazi W.B., Priyan K.S.S., Mosissa R. An efficient signal processing algorithm for detecting abnormalities in EEG signal using CNN. Contrast Media & Molecular Imaging. 2022. vol. 2022. DOI: 10.1155/2022/1502934.
25. Faiz M.M.U., Kale I. Removal of multiple artifacts from ECG signal using cascaded multistage adaptive noise cancellers. Array. 2022. vol. 14.
26. Prasad D.S., Chanamallu S.R., Prasad K.S. Optimized deformable convolution network for detection and mitigation of ocular artifacts from EEG signal. Multimedia Tools and Applications. 2022. vol. 81(21). pp. 30841–30879.
27. Behera S., Mohanty M.N. A Machine Learning Approach for Artifact Removal from Brain Signal. Computer Systems Science & Engineering. 2023. vol. 45(2).
28. Lopes F., Leal A., Medeiros J., Pinto M.F., Dourado A., Dümpelmann M., Teixeira C. Automatic electroencephalogram artifact removal using deep convolutional neural networks. IEEE Access. 2021. vol. 9. pp. 149955–149970.
29. Ghosh R., Phadikar S., Deb N., Sinha N., Das P., Ghaderpour E. Automatic eyeblink and muscular artifact detection and removal from EEG signals using k-nearest neighbor classifier and long short-term memory networks. IEEE Sensors Journal. 2023. vol. 23(5). pp. 5422–5436.

30. He H., Bai Y., Garcia E.A., Li S. ADASYN: Adaptive synthetic sampling approach for imbalanced learning. IEEE international joint conference on neural networks (IEEE world congress on computational intelligence). 2008. pp. 1322–1328.
31. Kiranyaz S., Ince T., Gabbouj M. Real-time patient-specific ECG classification by 1-D convolutional neural networks. IEEE transactions on biomedical engineering. 2015. vol. 63(3). pp. 664–675.
32. Saremi S., Mirjalili S., Lewis A. Grasshopper optimisation algorithm: theory and application. Advances in engineering software. 2017. vol. 105. pp. 30–47.
33. Kirkpatrick S., Gelatt Jr C.D., Vecchi M.P. Optimization by simulated annealing. Science. 1983. vol. 220(4598). pp. 671–680. DOI: 10.1126/science.220.4598.671.

Kokate Ashwini Amol — Professor, Department of electronics and telecommunication engineering, BRACT's Vishwakarma Institute of Information Technology. Research interests: electronics and telecommunications engineering. ashwini279@gmail.com; Kondhawa, Pune, India; office phone: +91(20)2695-0200.

Jadhav Tushar R. — Professor, Department of electronics and telecommunication engineering, BRACT's Vishwakarma Institute of Information Technology. Research interests: electronics and telecommunications engineering. tushar.jadhav@viit.ac.in; Kondhawa, Pune, India; office phone: +91(20)2695-0200.

УДК 004 **DOI** 10.15622/ia.24.5.6

А. Кокате, Т. Джадхав

НОВЫЙ ПОДХОД К УДАЛЕНИЮ АРТЕФАКТОВ ЭЭГ С ИСПОЛЬЗОВАНИЕМ ADASYN И ОПТИМИЗИРОВАННОЙ ИЕРАРХИЧЕСКОЙ ОДНОМЕРНОЙ СВЕРТОЧНОЙ НЕЙРОННОЙ СЕТИ 1D CNN

Кокате А., Джадхав Т. **Новый подход к удалению артефактов ЭЭГ с использованием ADASYN и оптимизированной иерархической одномерной сверточной нейронной сети 1D CNN.**

Аннотация. В нейронауке, нейроинженерии и биомедицинской инженерии электроэнцефалография (ЭЭГ) широко используется благодаря своей неинвазивности, высокому временному разрешению и доступности. Однако шум и физиологические артефакты, такие как сердечные, миогенные и глазные артефакты, часто искажают исходные данные ЭЭГ. Методы шумоподавления на основе глубокого обучения (DL) могут уменьшать или устранять эти артефакты, которые ухудшают ЭЭГ-сигнал. Несмотря на наличие этих методов, значительные артефакты всё ещё могут снижать эффективность анализа, что делает удаление шума основным требованием для точного анализа ЭЭГ. Кроме того, для эффективного удаления артефактов представлена оптимизированная иерархическая одномерная сверточная нейронная сеть (1D CNN). Для эффективного извлечения признаков иерархическая CNN сочетает в себе максимальное объединение, функцию активации ReLU и адаптивные сверточные окна. Для оптимизации параметров сети применяется алгоритм отжига кузнечика (AGA), что дополнительно улучшает устранение артефактов. Для обеспечения всестороннего исследования и сходимости к идеальным настройкам CNN, AGA сочетает точность тонкой настройки метода имитации отжига (SA) с глобальными исследовательскими возможностями алгоритма оптимизации кузнечика (GOA). Используя гибридный подход, сеть может более эффективно устранять артефакты на различных иерархических уровнях, что приводит к заметному улучшению чёткости сигнала и общей точности. Очищенные данные ЭЭГ представлены восстановленными элементами в последнем плотном слое иерархической одномерной CNN, использующей сигмоидальную функцию. Согласно экспериментальным результатам, предложенный метод достиг пикового отношения сигнала к шуму (PSNR) 29,5 дБ, средней абсолютной ошибки (MAE) 11,32, среднеквадратической ошибки (RMSE) 0,011 и коэффициента корреляции (CC) 0,93, что превосходит результаты предыдущих работ. Предложенный метод позволяет повысить точность удаления артефактов ЭЭГ, что является полезным дополнением к обработке биомедицинских сигналов и нейроинженерии.

Ключевые слова: электроэнцефалография (ЭЭГ), обработка сигналов, сверточная нейронная сеть (CNN), имитация отжига (SA), алгоритм оптимизации кузнечика (GOA).

Литература

1. Rashmi C.R., Shantala C.P. EEG artifacts detection and removal techniques for brain computer interface applications: a systematic review. International Journal of Advanced Technology and Engineering Exploration. 2022. vol. 9(88). pp. 354–383. DOI: 10.19101/IJATEE.2021.874883.
2. Yadav D., Yadav S., Veer K. A comprehensive assessment of Brain Computer Interfaces: Recent trends and challenges. Journal of Neuroscience Methods. 2020. vol. 346.

3. Mridha M.F., Das S.C., Kabir M.M., Lima A.A., Islam M.R., Watanobe Y. Brain-computer interface: Advancement and challenges. Sensors. 2021. vol. 21(17).
4. Satpathy R.B., Ramesh G.P. Advance approach for effective EEG artifacts removal. Recent Trends and Advances in Artificial Intelligence and Internet of Things. 2020. pp. 267–278.
5. Park Y., Han S.H., Byun W., Kim J.H., Lee H.C., Kim S.J. A real-time depth of anesthesia monitoring system based on deep neural network with large EDO tolerant EEG analog front-end. IEEE Transactions on Biomedical Circuits and Systems. 2020. vol. 14(4). pp. 825–837. DOI: 10.1109/TBCAS.2020.2998172.
6. Thomas J., Thangavel P., Peh W.Y., Jing J., Yuvaraj R., Cash S.S., Chaudhari R., Karia S., Rathakrishnan R., Saini V., Shah N., Srivastava R., Tan Y.-L., Westover B., Dauwels J. Automated adult epilepsy diagnostic tool based on interictal scalp electroencephalogram characteristics: A six-center study. International journal of neural systems. 2021. vol. 31(05). DOI: 10.1142/S0129065720500744.
7. Rasheed K., Qayyum A., Qadir J., Sivathamboo S., Kwan P., Kuhlmann L., O'Brien T., Razi A. Machine learning for predicting epileptic seizures using EEG signals: A review. IEEE reviews in biomedical engineering. 2021. vol. 14. pp. 139–155. DOI: 10.1109/RBME.2020.3008792.
8. Kapgate D. Future of EEG based hybrid visual brain computer interface systems in rehabilitation of people with neurological disorders. International Research Journal on Advanced Science Hub. 2020. vol. 2(6). pp. 15–20.
9. Raza H., Chowdhury A., Bhattacharyya S. Deep learning based prediction of EEG motor imagery of stroke patients' for neuro-rehabilitation application. International Joint Conference on Neural Networks (IJCNN). IEEE. 2020. pp. 1–8.
10. Mumtaz W., Rasheed S., Irfan A. Review of challenges associated with the EEG artifact removal methods. Biomedical Signal Processing and Control. 2021. vol. 68.
11. Anwer S., Li H., Antwi-Afari M.F., Mirza A.M., Rahman M.A., Mehmood I., Wong A.Y.L. Evaluation of Data Processing and Artifact Removal Approaches Used for Physiological Signals Captured Using Wearable Sensing Devices during Construction Tasks. Journal of Construction Engineering and Management. 2024. vol. 150(1).
12. Zangeneh Soroush M., Tahvilian P., Nasirpour M.H., Maghooli K., Sadeghniiat-Haghighi K., Vahid Harandi S., Jafarnia Dabanloo N. EEG artifact removal using sub-space decomposition, nonlinear dynamics, stationary wavelet transform and machine learning algorithms. Frontiers in Physiology. 2022. vol. 13. DOI: 10.3389/fphys.2022.910368.
13. Islam M.K., Rastegarnia A., Sanei S. Signal artifacts and techniques for artifacts and noise removal. Signal Processing Techniques for Computational Health Informatics. 2021. pp. 23–79.
14. Mahmood D., Nisar H., Voon Y.V. Removal of physiological artifacts from electroencephalogram signals: a review and case study. IEEE 9th Conference on Systems, Process and Control (ICSPC). 2021. pp. 141–146.
15. Jindal K., Upadhyay R., Singh H.S. Application of hybrid GLCT-PICA de-noising method in automated EEG artifact removal. Biomedical Signal Processing and Control. 2020. vol. 60.
16. Kotte S., Dabbakuti J.K. Methods for removal of artifacts from EEG signal: A review. In Journal of Physics: Conference Series. IOP Publishing. 2020. vol. 1706. no. 1.
17. Ranjan R., Sahana B.C., Bhandari A.K. Ocular artifact elimination from electroencephalography signals: A systematic review. Biocybernetics and Biomedical Engineering. 2021. vol. 41(3). pp. 960–996.
18. Sheela P., Puthankattil S.D. A hybrid method for artifact removal of visual evoked EEG. Journal of neuroscience methods. 2020. vol. 336.

19. Kaur C., Bisht A., Singh P., Joshi G. EEG Signal denoising using hybrid approach of Variational Mode Decomposition and wavelets for depression. Biomedical Signal Processing and Control. 2021. vol. 65.
20. Vallabhaneni R.B., Sharma P., Kumar V., Kulshreshtha V., Reddy K.J., Kumar S.S., Kumar V.S., Bitra S.K. Deep learning algorithms in EEG signal decoding application: a review. IEEE Access. 2021. vol. 9. pp. 125778–125786. DOI: 10.1109/ACCESS.2021.3105917.
21. Pawar D., Dhage S.N. Feature extraction methods for electroencephalography based brain-computer interface: a review. Entropy. 2020. vol. 1(4).
22. Ahmed M.A., Qi D., Alshemmary E.N. Effective hybrid method for the detection and rejection of electrooculogram (EOG) and power line noise artifacts from electroencephalogram (EEG) mixtures. IEEE Access. 2020. vol. 8. pp. 202919–202932.
23. Mathe M., Padmaja M., Krishna B.T. Intelligent approach for artifacts removal from EEG signal using heuristic-based convolutional neural network. Biomedical Signal Processing and Control. 2021. vol. 70. DOI: 10.1016/J.BSPC.2021.102935.
24. Syamsundararao T., Selvarani A., Rathi R., Vini Antony Grace N., Selvaraj D., Almutairi K., Alonazi W.B., Priyan K.S.S., Mosissa R. An efficient signal processing algorithm for detecting abnormalities in EEG signal using CNN. Contrast Media & Molecular Imaging. 2022. vol. 2022. DOI: 10.1155/2022/1502934.
25. Faiz M.M.U., Kale I. Removal of multiple artifacts from ECG signal using cascaded multistage adaptive noise cancellers. Array. 2022. vol. 14.
26. Prasad D.S., Chanamallu S.R., Prasad K.S. Optimized deformable convolution network for detection and mitigation of ocular artifacts from EEG signal. Multimedia Tools and Applications. 2022. vol. 81(21). pp. 30841–30879.
27. Behera S., Mohanty M.N. A Machine Learning Approach for Artifact Removal from Brain Signal. Computer Systems Science & Engineering. 2023. vol. 45(2).
28. Lopes F., Leal A., Medeiros J., Pinto M.F., Dourado A., Dümpelmann M., Teixeira C. Automatic electroencephalogram artifact removal using deep convolutional neural networks. IEEE Access. 2021. vol. 9. pp. 149955–149970.
29. Ghosh R., Phadikar S., Deb N., Sinha N., Das P., Ghaderpour E. Automatic eyeblink and muscular artifact detection and removal from EEG signals using k-nearest neighbor classifier and long short-term memory networks. IEEE Sensors Journal. 2023. vol. 23(5). pp. 5422–5436.
30. He H., Bai Y., Garcia E.A., Li S. ADASYN: Adaptive synthetic sampling approach for imbalanced learning. IEEE international joint conference on neural networks (IEEE world congress on computational intelligence). 2008. pp. 1322–1328.
31. Kiranyaz S., Ince T., Gabbouj M. Real-time patient-specific ECG classification by 1-D convolutional neural networks. IEEE transactions on biomedical engineering. 2015. vol. 63(3). pp. 664–675.
32. Saremi S., Mirjalili S., Lewis A. Grasshopper optimisation algorithm: theory and application. Advances in engineering software. 2017. vol. 105. pp. 30–47.
33. Kirkpatrick S., Gelatt Jr C.D., Vecchi M.P. Optimization by simulated annealing. Science. 1983. vol. 220(4598). pp. 671–680. DOI: 10.1126/science.220.4598.671.

Кокате Ашвини Амол — профессор, факультет электроники и телекоммуникационной инженерии, Институт информационных технологий Вишвакармы. Область научных интересов: электроника и телекоммуникационная инженерия. ashwini279@gmail.com; Кондхава, Пуна, Индия; р.т.: +91(20)2695-0200.

Джадхав Тушар Р. — профессор, факультет электроники и телекоммуникационной инженерии, Институт информационных технологий Вишвакармы. Область научных интересов: электроника и телекоммуникационная инженерия. tushar.jadhav@viit.ac.in; Кондхава, Пуна, Индия; р.т.: +91(20)2695-0200.